Open Access Library Journal
2024, Volume 11, e11756
ISSN Online: 2333-9721
ISSN Print: 2333-9705

Coordination Studies of the [13]aneN$_4$ with Chromophoric Groups

Rim Zaari Jabri[1,2], Stephane Brandes[2], Yoann Rousselin[2], Christine Goze[2], Abdellah Zrineh[1], Franck Denat[2]

[1]Laboratoire de Physique Générale, Faculté des Sciences, Université Mohammed V de Rabat, Rabat, Morocco
[2]ICMUB, UMR 5260, CNRS, Université de Bourgogne, Dijon, France
Email: rimjabri@gmail.com

How to cite this paper: Jabri, R.Z., Brandes, S., Rousselin, Y., Goze, C., Zrineh, A., Denat, F. (2024) Coordination Studies of the [13]aneN$_4$ with Chromophoric Groups. *Open Access Library Journal*, **11**: e11756.
https://doi.org/10.4236/oalib.1111756

Received: May 28, 2024
Accepted: July 12, 2024
Published: July 15, 2024

Abstract

We report here a complete study of coordination of the 5-aminomethyl-[13]aneN$_4$ with chromophoric groups (anthracene, pyrene and naphtalene) by four metals: Zn(II), Cu(II), Ni(II) and Cr(III). We aim to study the effect of the C-functionalization of the macrocycle on the stability of the metal complexes and the size of the metal impact on the quenching of fluorescence of the chromophoric groups. The results obtained by spectrometry, EPR and X-ray of the metal complexes confirm that the copper is pentacoordinate by four nitrogen atoms of the macrocycle, but the chromium and nickel complexes are hexacoordinated in octahedral geometry. For all metal complexes, the coordination of the nitrogen atom is observed with the primary amine function.

Subject Areas

Organic Chemistry

Keywords

Spectroscopy, Complexation, Fluorescence, Metal Complex, X-Ray Diffraction, Single Crystal Structure, 5-Aminomethyl-[13]aneN$_4$, RPE Spectra, Metal Detection, Energy Transfer, Photoinduced Electron Transfer

1. Introduction

Fluorescent molecular probes have attracted great interest in recent years. Thanks to their applications in several chemicals, environmental and biological. [1] [2] An efficient and selective detection method for metal cations is performed by a combination of coordination chemistry and fluorescence spectroscopy.

Compounds associating an entity for recognizing the target cation "ionophore" with a fluorescent optical transducer "fluorophore" via a spacer or not are likely to meet the sensitivity and selectivity criteria. In recent years, methods of detection based on such compounds have been the subject of a great deal of work. [3]-[5] The photophysical modifications of the fluorophore during the presence of the cation in the recognition entity are due to a disruption of the fluorophore by a phenomenon photoinduced (shift of spectra and/or variation of quantum yield by transfer photoinduced electron, charge or energy, formation or disappearance of excimers, etc.). In this context, we were interested in fluorescent probes based on C-functionalized tetraazacyclocanes.

One of the objectives of the functionalization of tetraazacycloalkanes is the anchoring of the macrocycle on a solid support or an antibody. [6] C-functionalization consists of introducing a functional group onto a carbon atom of the macrocyclic skeleton, thus making it possible to retain the four secondary amine functions of the macrocycle. One way to access such C-functionalized macrocycles is to use a derivative of diethyl malonate. [7] The coordination of an amine group "pending" to a metal ion in an aqueous solution depends on pH. This molecular movement can be detected by the introduction of a fluorophore group on the amine function, the fluorescence is affected by amine coordination [8]. We considered studying the photophysical properties of new metallic cations based fluoro ionophores [9], in order to study the coordination of these metals series for application and use as a metal detector for industry waste water treatment.

2. Materials and Methods

2.1. Synthesis of cis-(9b,9c-Dimethyldecahydro-2a,4a,7a,9a-tetraazacyclopenta[cd]-phenylen-1-yl)methanamine (Ligand 1) [10] [11]

A solution of 2,3-butanedione (27.45 g, 0.319 mol) in acetonitrile (10 mL) was added to a solution of N,N-bis(aminoethyl)propane-1,3-diamine (51.1 g, 0.319 mmol) in acetonitrile (1.5 L) at 0˚C. The mixture was stirred at this temperature for 2 h. Benzotriazole (38.1 g, 1 equiv.) and K_2CO_3 (88.2 g, 2 equiv.) were added. A solution of 50% chloroacetaldehyde in water (50.1 g, 0.319 mol) was slowly added at 0˚C and the resulting mixture was stirred overnight at room temperature. Then the solution was filtered through Celite and washed with acetonitrile (100 mL). The filtrate was evaporated. The resulting solid was dissolved in CH_2Cl_2 (500 mL). After filtration, the organic phase was washed with a 3 M NaOH solution (200 mL). After extraction, the organic phase was dried with $MgSO_4$ and the solvent was evaporated. The residual brown solid was purified by aluminium oxide chromatography (eluent: CH_2Cl_2). A solution of this compound (40.73 g, 0.156 mol) in dry THF (50 mL) was slowly added to a suspension of $LiAlH_4$ (11.8 g, 0.31 mol) in THF (200 mL) under nitrogen at −78˚C. The resulting mixture was stirred overnight. Ethyl acetate (100 mL) and then water (25 mL) were carefully added. After removal of the solvent, the residual white-grey solid was taken up in chloroform (2 × 200 mL) and insoluble

products were eliminated by filtration. Compound 1 was obtained as a colorless oil (yield 32.16 g, 78%). ^{1}H NMR (300 MHz, $CDCl_3$, 300 K): δ = 1.04 (s, 3 H), 1.12 (s, 3 H), 1.27 (s, 2.9 H), 1.28 (s, 2.9 H), 1.76 (m, 1.3 H), 2.2 - 3.6 (m, 26.6 H) ppm. $^{13}C\{^{1}H\}$ NMR (75 MHz, $CDCl_3$, 300 K): δ = 11.9, 12.3 (×2), 13.4 (CH_3), 18.7, 25.8 (CH_2-β), 44.8, 44.9, 45.7, 45.9, 46.5, 46.6, 47.2 (×2), 48.0, 48.3, 48.4, 49.4, 50.0, 50.1, 51.0, 51.1 (CH_2-α), 61.8, 68.1 (C-H), 73.2, 73.4, 79.3, 80.5 (N-C-N) ppm. MS (MALDI-TOF): m/z = 265.82 $[M]^+$.

2.2. Synthesis of (1,4,7,10-Tetraazacyclotridecan-5-yl)methanamine (Ligand 2) [10] [11]

A solution of 35% hydrochloric acid (107 mL, 1.2 mol) was added to a solution of 1 (32.16 g, 0.12 mol) in ethanol (200 mL). The resulting mixture was heated at reflux for 4 h. After cooling, the solution was filtered and washed with ethanol (50 mL) and then diethyl ether (100 mL). The solid was dissolved in a saturated 15 M NaOH solution (10 mL). After extraction with chloroform (2 × 150 mL), the organic phase was dried with $MgSO_4$ and the solvent was evaporated. Compound **2** was obtained as a white solid; yielding 11.02 g, 42%. ^{1}H NMR (300 MHz, $CDCl_3$): δ = 1.63 (m, 2 H), 1.87 (s, 6 H), 2.67 - 2.76 (m, 17 H) ppm. $^{13}C\{^{1}H\}$ NMR (75 MHz, $CDCl_3$): δ = 28.9 (CH_2-β), 44.3, 46.2, 47.7, 49.0, 49.0, 49.7, 49.8, 50.8 (CH_2-α), 59.0 (CH) ppm. MS (MALDI-TOF): m/z = 215.68 $[M]^+$. $C_{10}H_{25}N_5 \cdot 0.2H_2O$ (221.62): calculated. C 54.86, H 11.69, N 31.99; found C 55, H 11.57, N 31.81.

2.3. Synthesis of N-((1,4,7,10-Tetraazacyclotridecan-5yl)methyl)-1-(anthracen-9-yl)methanamine (3b) :[9]

To a solution of 350 mg (1.6 mmol) of compound **2** in 50 mL of ethanol is added 411 mg (1.6 mmol) of 9-bromoanthracene. The mixture is stirred at ambient temperature for 4 h. $NaBH_4$ (0.6 g, 16 mmol, 10 equivalents) is then added and the mixture is brought to reflux. After 24 h, the solvent is evaporated off and the solid is dissolved in 50 mL of chloroform and then filtered. After evaporation of the solvent, the solid is dissolved in 50 mL of cyclohexane and then filtered and the solvent is evaporated off. Compound **3b** is obtained in the form of yellow oil (486 mg, 1.2 mmol, Yield = 75%). MALDI-TOF: m/z = 405.86 $[M]^{+\bullet}$; 405.25 calculated for $C_{25}H_{35}N_5$, UV-vis. (CH_3OH): λ_{max}/nm (ε/M^{-1} cm^{-1}) = 385 (9135). ^{1}H NMR ($CDCl_3$, 300 MHz): 8.18 (m, 3 H); 7.78 (d, J = 8.5 Hz, 1 H); 7.31 (d, J = 8.3 Hz, 1 H); 7.35 (m, 4 H); 4.72 (s, 2 H); 2.45 (m, 22 H); 1.69 (m, 2 H). RMN $^{13}C\{^{1}H\}$ ($CDCl_3$, 75 MHz): 142.8; 135.1 ;132.4; 128.9; 125.2; 125.2; 124.8; 124.4; 123.3; 120.5; 57.6; 53.2; 51.1; 49.8; 49.6; 49.0; 48.8; 47.4; 46.2; 28.4.

2.3.1. Synthesis of $[Zn(3b)](C_2H_3O_2)_2$

$Zn(C_2H_3O_2)_2.2H_2O$ (279.6 mg, 1.27 mmol) is added to a solution of compound **3b** (516 mg, 1.27 mmol) in methanol (30 mL). The mixture is stirred at temperature ambient for 3 hours. The solution is filtered and then evaporated.

The solid obtained is washed with acetonitrile. The complex is obtained in the form of an orange solid (530 mg, 0.90 mmol, yield = 71%). MALDI-TOF: m/z = 469 [M-2 $C_2H_3O_2$]$^+$; 469.22 calculated for $C_{25}H_{35}N_5Zn$. UV-vis. (CH_3OH): λ_{max} /nm (ε/M^{-1} cm^{-1}) = 366 (7122). ^1H NMR (CD_3OD, 300 MHz): 8.30 (m, 3 H); 7.88 (d, J = 8.5 Hz, 1 H); 7.81 (d, J = 8.3 Hz, 1 H); 7.45 (m, 4 H); 4.93 (s, 6 H); 4.62 (m, 2 H); 2.55 (m, 15 H); 1.59 (m, 2 H). $^{13}C\{^1H\}$ NMR (CD_3OD, 75.4 MHz): 180.7 ;132.9; 132.5; 131.8; 131.6; 130.1; 129.9; 128.8; 128.5; 127.2; 127.0; 126.2; 126.0; 125.4; 125.3; 57.1; 56.9; 51.4; 50.7; 45.8; 45.2; 43.7; 28.4; 23.2. Elemental analysis $C_{25}H_{35}N_5Zn(C_2H_3O_2)_2$. $2H_2O$: calculated: C 55.72; N 11.20; H 7.26; found: C 55.39; N 11.36; H 7.22.

2.3.2. Synthesis of [Ni(3b)]$(C_2H_3O_2)_2$

$Ni(C_2H_3O_2)_2$. $4H_2O$ (306 mg, 1.23 mmol) is added to a solution of compound 3b (500 mg, 1.23 mmol) in methanol (20 mL). The mixture is brought to reflux for 2 h. The purple solution is evaporated and then washed with acetonitrile and the complex is obtained in the form of a brown solid (605 mg, 1.04 mmol, yield = 85%). MALDI-TOF: m/z = 463[M-2 $C_2H_3O_2$]$^+$; 463.22 calculée pour $C_{25}H_{35}N_5Ni$. UV-vis. (CH_3OH): λ_{max} /nm (ε/M^{-1} cm^{-1}) = 552 (18), 367 (7255). Elemental analysis $C_{25}H_{35}N_5Ni(C_2H_3O_2)_2$. $2H_2O$: calculated: C 56.33; N 11.33; H 7.33; found: C 56.45; N 11.13; H 7.12.

2.3.3. Synthesis of [Cu(3b)]Cl_2

$CuCl_2$ (140 mg, 0.98 mmol) is added to a solution of compound **3b** (700 mg, 0.98 mmol) in methanol (30 mL). The mixture is brought to reflux for 2 h. The complex obtained is precipitated by adding diethyl ether, filtered, washed with dichloromethane and diethyl ether then dried (423 mg, 0.784 mmol, yield = 80%). MALDI-TOF: m/z = 503 [M- Cl]$^+$; 503.19 calculated for $C_{25}H_{35}ClCuN_5$. UV-vis. (CH_3OH): λ_{max}/nm (ε/M^{-1} cm^{-1}) = 582 (145), 365 (6933). Elemental analysis $C_{25}H_{35}N_5CuCl_2$. $3H_2O$: calculated: C 50.54; N 11.79; H 6.96; found: C 50.14; N 11.80; H 6.89.

2.3.4. Synthesis of [Cr(3b)]Cl_3

$CrCl_3(THF)_3$ (1.13 mg, 3 mmol) is added to a solution of compound **3b** (1.29 mg, 3.18 mmol) in distilled DMF (7 mL). The mixture is brought to reflux under nitrogen for 50 min. The precipitate formed is filtered off and then washed with acetone and diethyl ether. The final complex is obtained in the form of a crystalline solid of violet color (1.34 mg, 2.38 mmol, Yield = 75%). ESI: m/z = 527,16 [M- Cl]$^+$; 527.17 calculated for $C_{25}H_{35}Cl_2$ CrN_5. UV-vis. (CH_3OH): λ_{max} /nm (ε/M^{-1} cm^{-1}) = 537 (330), 368 (6844). Elemental analysis $C_{25}H_{35}N_5CrCl_3$. $3H_2O$: calculated: C 46.36; N 11.30; H 6.69; found: C 46.09; N 11.24; H 6.74.

2.4. Synthesis of N-((1,4,7,10-Tetraazacyclotridecan-5-yl)methyl)-1-(pyren-2-yl)methanamine (4b): [9]

To a solution of 350 mg (1.6 mmol) of compound **2** in 50 mL of ethanol is

added 450 mg (1.6 mmol) of 2-bromopyrene. The mixture is stirred at ambient temperature for 4 h. $NaBH_4$ (0.6 g, 16 mmol, 10 equivalents) is then added and the mixture is brought to reflux. After 24 h, the solvent is evaporated off and the solid is dissolved in 50 mL of chloroform and then filtered. After evaporation of the solvent, the solid is dissolved in 50 mL of cyclohexane and then filtered and the solvent is evaporated off. Compound **4b** is obtained in the form of yellow oil (515 mg, 1.2 mmol, Yield = 75%). MALDI-TOF: m/z = 429.88 $[M]^{+\bullet}$; 429.27 calculated for $C_{27}H_{35}N_5$, UV-vis. (CH_3OH): λ_{max}/nm (ε/M^{-1} cm^{-1}) = 341 (35,185). ^1H NMR ($CDCl_3$, 300 MHz): 8.40 (m, 1 H); 7.92 (m, 8 H); 4.42 (s, 2 H); 3.54 – 1.92 (m, 22 H); 1.60 (m, 2 H). $^{13}C\{^1H\}$ NMR ($(CD_3)_2SO$, 75.4 MHz): 130.8; 126.8; 126.3; 125.8; 124.7; 123.5; 123.4; 123.1; 122.9; 121.2; 120.0; 119.6; 118.1; 117.5; 51.8; 49.7; 48.9; 48.6; 48.4; 48.1; 47.7; 47.6; 47.3; 27.9.

2.4.1. Synthesis of $[Zn(4b)](C_2H_3O_2)_2$

$Zn(C_2H_3O_2)_2.2H_2O$ (219.5 mg, 1.16 mmol) is added to a solution of compound **4b** (500 mg, 1.16 mmol) in methanol (50 mL). The mixture is brought to reflux for 1 hour. The solution is filtered and then evaporated. The solid obtained is washed with dichloromethane, thus making it possible to obtain a yellow solid (551 mg, 0.90 mmol, Yield = 78%). MALDI-TOF: m/z = 493.91 $[M\text{-}2C_2H_3O_2]^+$; 493.22 calculated for $C_{27}H_{35}N_5Zn$. UV-vis. (CH_3OH): λ_{max}/nm (ε/M^{-1} cm^{-1}) = 342 (37,076). ^1H NMR ($(CD_3)_2SO$, 300 MHz): 8.52 (m, 1 H); 8.13 (m, 8 H); 4.42 (s, 1 H); 3.99 (m, 2 H); 3.44 (s, 5 H); 3.16 (s, 2 H); 2.73 (m, 9 H); 2.19 (m, 5 H); 1.74 (s, 6 H); 1.34 (m, 2 H). $^{13}C\{^1H\}$ NMR ($(CD_3)_2SO$, 75.4 MHz): 134.8; 130.8; 130.3; 130.0; 128.7; 127.5; 127.4; 127.1; 126.9; 126.2;125.0; 124.6; 124.1; 124.0; 55.5; 51.4; 49.7; 49.6; 48.9; 48.5; 47.8; 47.7; 47.4; 47.3; 40.3; 23.9. Elementalanalysis $C_{27}H_{35}N_5Zn(C_2H_3O_2)_2$, $4H_2O$: calculated: C 54.34; N 10.22; H 7.21; found: C 54.40; N 10.27; H 6.51.

2.4.2. Synthesis of $[Ni(4b)](C_2H_3O_2)_2$

$Ni(C_2H_3O_2)_2.4H_2O$ (288.67 mg, 1.16 mmol) is added to a solution of compound **4b** (500 mg, 1.16 mmol) in methanol (50 mL). The mixture is brought to reflux for 3 h. The purple solution is evaporated. The solid obtained is then redissolved in dichloromethane and then filtered in order to remove the insoluble impurities. Finally, the solution is evaporated and the complex is recovered in the form of a purple solid (539 mg, 0.89 mmol, Yield = 77%). MALDI-TOF: m/z = 487 $[M\text{-}2C_2H_3O_2]^+$; 487,22 calculated for $C_{27}H_{35}N_5Ni$. UV-vis. (CH_3OH): λ_{max} /nm (ε/M^{-1} cm^{-1}) = 535 (36), 343 (39,417). Elemental analysis $C_{27}H_{35}N_5Ni(C_2H_3O_2)_2$. $3H_2O$: calculated: C 56.38; N 10.60; H 7.17; found: C 56.93; N 10.67; H 6.98.

2.4.3. Synthesis of $[Cu(4b)]Cl_2$

$CuCl_2$ (156.4 mg, 1.16 mmol) is added to a solution of compound **4b** (500 mg, 1.16 mmol) in methanol (50 mL). The mixture is brought to reflux for 2 h. The complex is precipitated by adding diethyl ether then filtered and washed with

dichloromethane (20 mL). The expected complex is obtained in the form of a blue solid (490 mg, 0.87 mmol, yield = 75%). MALDI-TOF: m/z = 492 $[M\text{-}2Cl]^+$; 492.22 calculée pour $C_{27}H_{35}CuN_5$. UV-vis. (CH_3OH): λ_{max}/nm (ε/M^{-1} cm^{-1}= 596 (230), 342 (37,751). Elemental analysis $C_{27}H_{35}N_5CuCl_2.CH_2Cl_2$: calculated: C 51.80; N 10.79; H 5.75; found: C 51.20; N 10.82; H 5.52.

2.4.4. Synthesis of $[Cr(4b)]Cl_3$

$CrCl_3(THF)_3$ (434.62 mg, 1.16 mmol) is added to a solution of compound **4b** (500 mg, 1.16 mmol) in DMF (10 mL). The mixture is brought to reflux under nitrogen for 1 hour. The precipitate formed is filtered off and then washed with acetone and diethyl ether (611 mg, 1.04 mmol, Yield = 90%). MALDI-TOF: m/z = 516,83 $[M\text{-}2Cl]^+$; 516.20 calculated for $C_{27}H_{35}ClCrN_5$. UV-vis. (CH_3OH): λ_{max} /nm (ε/M^{-1} cm^{-1}) = 533 (148), 342 (18,208). Elemental analysis $C_{27}H_{35}Cl_3CrN_5$. $2H_2O$: calculated: C 55.16; N 11.91; H 6.00; found: C 55.07; N 12.11; H 5.95.

2.5. Synthesis of N-((1,4,7,10-tétraazacyclotridécan-5-yl)méthyl)-1-(naphthalèn-1-yl)méthanamine (5b): [9]

To a solution of 350 mg (1.6 mmol) of compound **2** in 50 mL of ethanol is added 250 mg (1.6 mmol) of 1-naphthaldehyde. The mixture is stirred at ambient temperature for 4 h. $NaBH_4$ (0.6 g, 16 mmol, 10 equivalents) is then added and the mixture is brought to reflux. After 24 h, the solvent is evaporated off and the solid is dissolved in 50 mL of chloroform and then filtered. After evaporation of the solvent, the solid is dissolved in 50 mL of cyclohexane and then filtered and the solvent is evaporated off. Compound **5b** is obtained in the form of yellow oil (512 mg, 1.44 mmol, Yield = 90%). MALDI-TOF: m/z = 355.88 $[M]^{+\bullet}$; 355.27 calculated for $C_{21}H_{33}N_5$, UV-vis. (CH_3OH): λ_{max}/nm (ε/M^{-1} cm^{-1}) = 283 (6746). ^1H NMR ($CDCl_3$, 300 MHz): 8.10 (d, J = 8.2 Hz, 1 H); 7.82 (d, J = 8.2 Hz, 1 H); 7.73 (d, J = 8.2 Hz, 1 H); 7.43 (m, 4 H); 4.9 (s, 2 H); 2.63 (m, 22 H); 1.69 (m, 2 H). $^{13}C\{^1H\}$ NMR ($CDCl_3$, 75.4 MHz): 135.1; 132.9; 130.9; 127.7; 126.8; 125.2; 125.0; 124.7; 124.4; 122.9; 56.0; 51.4; 51.2; 50.2; 48.7; 48.6; 48.2; 47.5; 46.5; 45.0; 27.3.

2.5.1. Synthesis of $[Zn(5b)](C_2H_3O_2)_2$

$Zn(C_2H_3O_2)_2$. $2H_2O$ (326.8 mg, 1.49 mmol) is added to a solution of compound **5b** (530 mg, 1.49 mmol) in methanol (50 mL). The mixture is stirred at ambient temperature for 3 h. The solution is then filtered and then evaporated. The solid obtained is dissolved in acetonitrile and then filtered again to remove insoluble impurities and the solution is evaporated. The complex is obtained in the form of a yellow solid (593 mg, 1.10 mmol, yield = 74%). MALDI-TOF: m/z = 419 $[M\text{-}2C_2H_3O_2]^+$; 419.20 calculated for $C_{21}H_{33}N_5Zn$. UV-vis. (CH_3OH): λ_{max} /nm (ε/M^{-1} cm^{-1}) = 283 (2098). ^1H NMR ($(CD_3)_2SO$, 300 MHz): 8.22 (d, J = 8.2, 1 H); 7.92 (d, J = 8.2, 1 H); 7.83 (d, J = 8.2, 1 H); 7.53 (m, 4 H); 3.72 (s, 10 H); 2.73 (m, 11 H); 2.33 (m, 3 H); 1.81 (s, 6 H); 1.56 (m, 2 H). $^{13}C\{^1H\}$ NMR ($(CD_3)_2SO$, 75.4

MHz): 175.4; 136.1; 133.3; 128.3; 127.8; 127.4; 126.4; 126.2; 125.8; 125.6; 125.3; 124.1; 61.7; 61.1; 55.1; 54.5; 51.1; 49.9; 48.5; 47.8; 42.3; 29.1; 27.1; 23.2. Elemental analysis $C_{21}H_{33}N_5Zn(C_2H_3O_2)_2$, $2H_2O$: calculated: C 52.22; N 12.18; H 7.54; found: C 51.70; N 12.08; H 7.46.

2.5.2. Synthesis of $[Ni(5b)](C_2H_3O_2)_2$

$Ni(C_2H_3O_2)_2{\cdot}4H_2O$ (216 mg, 0.868 mmol) is added to a solution of compound **5b** (309 mg, 0.868 mmol) in methanol (20 mL). The mixture is brought to reflux for 3 h. The violet solution is then evaporated. The solid obtained is dissolved in acetonitrile and then filtered again to remove insoluble impurities and the solution is evaporated. Finally, the solution is evaporated and the complex is obtained in the form of a purple solid (323 mg, 0.607 mmol, Yield = 70%). MALDI-TOF: m/z = 413.89 $[M\text{-}2\ C_2H_3O_2]^+$; 413.21 calculée pour $C_{21}H_{33}N_5Ni$. UV-vis. (CH_3OH): λ_{max}/nm ($\varepsilon/M^{-1}\ cm^{-1}$) = 563 (16), 282 (6807). Elemental analysis $C_{21}H_{33}N_5Ni(C_2H_3O_2)_2{\cdot}3H_2O$: calculated: C 51.21; N 11.94; H 7.74; found: C 51.41; N 11.65; H 7.55.

2.5.3. Synthesis of $[Cu(5b)]Cl_2$

$CuCl_2$ (114.13 mg, 0.848 mmol) is added to a solution of compound **5b** (302 mg, 0.848 mmol) in methanol (50 mL). The mixture is brought to reflux for 3 h. The complex is obtained by precipitation in diethyl ether in the form of a blue solid (282 mg, 0.576 mmol, Yield = 68%). MALDI-TOF: m/z = 418.89 $[M\text{-}2Cl]^+$; 418.20 found for $C_{21}H_{33}CuN_5$, UV-vis. (CH_3OH): λ_{max}/nm ($\varepsilon/M^{-1}\ cm^{-1}$) = 585 (215), 282 (8652). Elemental analysis $C_{21}H_{33}N_5CuCl_2$. $2H_2O$: calculated: C 47.95; N 13.31; H 7.09; found: C 48.03; N 12.95; H 7.39.

2.5.4. Synthesis of $[Cr(5b)]Cl_3$

$CrCl_3(THF)_3$ (324.4 mg, 0.857 mmol) is added to a solution of compound **5b** (305 mg, 0.857 mmol) in DMF (10 mL). The mixture is brought to reflux under nitrogen for 1 hour. The precipitate formed is filtered off and then washed with acetone and diethyl ether (376 mg, 0.668 mmol, Yield = 78%). MALDI-TOF: m/z = 442.88 $[M\text{-}2Cl]^+$; 442.18 calculated for $C_{21}H_{33}ClCrN_5$, UV-vis.(CH_3OH): λ_{max} /nm ($\varepsilon/M^{-1}\ cm^{-1}$) = 534 (123), 396 (330), 284 (5652). Elemental analysis $C_{21}H_{33}N_5CrCl_3$. $3H_2O$: calculated: C 44.41; N 12.33; H 6.92; found: C 44.85; N 12.45; H 7.02.

3. Discussion

3.1. Synthesis of Metal Complexes of Ligands

In order to study the coordination of transition metals by compounds **3b**, **4b** and **5b**, we have synthesized the copper (II), zinc (II), nickel (II) and chromium (III) complexes of these compounds (Scheme 1).

The complexes of copper (II) and nickel (II) were obtained by reacting the salt metals and macrocycles in methanol at reflux for two hours. The complexes of zinc (II) were synthesized by reacting the metal salt and the macrocycles in the methanol at room temperature for three hours.

Finally, the metallation of compounds **3b**, **4b** and **5b** by chromium (III) was carried out according to the method used by Tobe and Ferguson [12]. At reflux of DMF, the Cr (III) complex is formed with the appearance of an intense purple color after a few minutes. Structures of crystallographic complexes of [Ni (**2**)]$^{2+}$, [Cu (**2**)]$^{2+}$ and [Cr (**2**)]$^{3+}$ were obtained by X-ray diffraction.

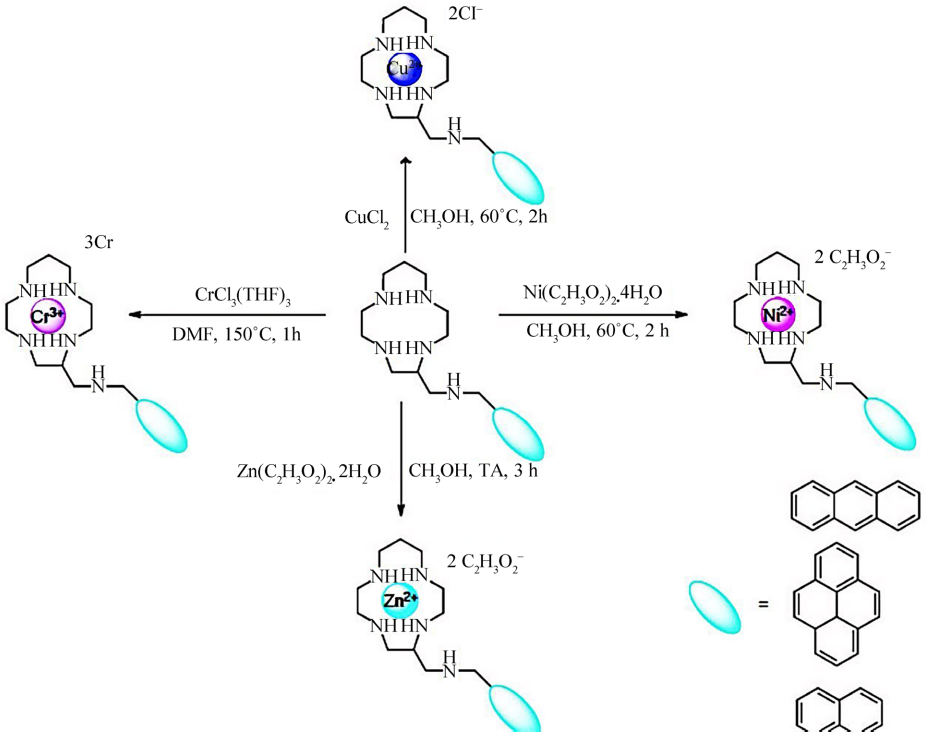

Scheme 1. Complexation of metals by the ligands.

The formation of metal complexes was confirmed by elemental analysis, mass spectrometry and by NMR for the zinc (II) complexes (cf. Experimental part).

The coordination geometries were studied by different spectrometric methods and spectroscopic (by RPE for Cu^{2+} complexes).

3.2. Photophysical Studies of Complexes in Methanol

The fluorescence emission spectra of compounds **3b**, **4b** and **5b** and their metal complexes were recorded in methanol at concentrations of 10^{-5} M for compounds **3b** and **5b** and 10^{-6} M for compound **4b**.

The superposition of the emission spectra of the metal complexes of compound **3b** is shown in **Figure 1**.

The fluorescence intensity of compound **3b** decreases after complexation with Cr^{3+}, Ni^{2+} and Cu^{2+} with quantum yields of φ = 0.02; 0.014 and 0.008 respectively. In contrast, complexation with Zn^{2+} leads to an increase in the fluorescence intensity of the anthracene group in the excited state with a quantum yield of $\varphi = 0.10$.

In **Figure 2**, we represent the emission spectra of compound **4b** and its metal

complexes.

Excitation of the pyrene group of compound **4b** and its metal complexes in methanol shows a decrease in fluorescence intensity at the wavelength of 376nm after the addition of Ni^{2+}, Cr^{3+} and Cu^{2+}. However, the addition of the Zn^{2+} metal ion to compound **4b** allows the fluorescence intensity to be increased (Figure 2).

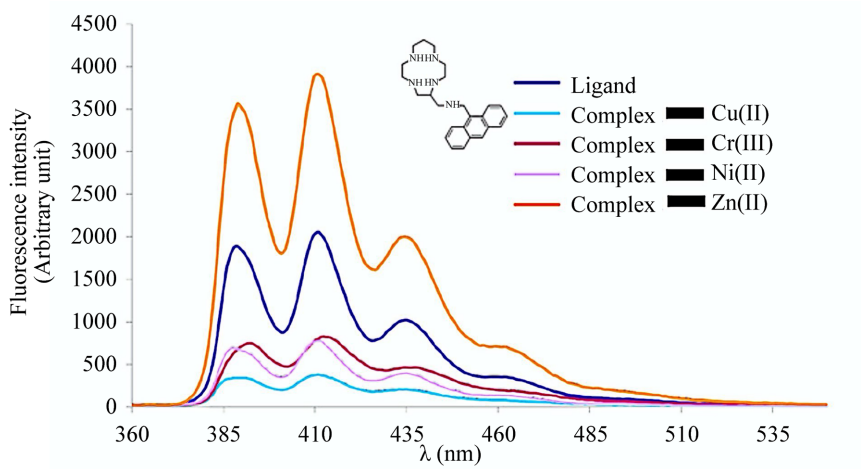

Figure 1. Emission spectra of the complexes of compound 3b in methanol, [10^{-5} M], λ_{ex} = 345 nm.

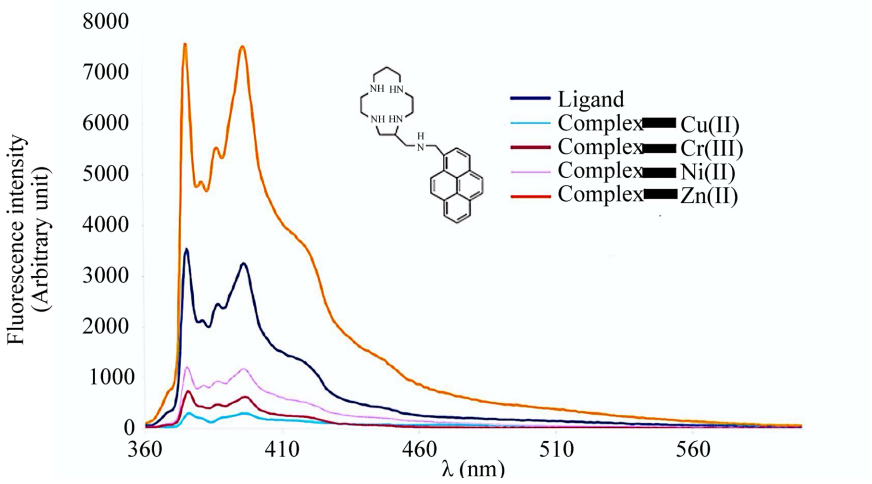

Figure 2. Emission spectra of compounds of compound **4b** in methanol, [10^{-6} M], λ_{ex} = 340 nm.

With regard to compound **5b**, we obtain results comparable to those observed for the two compounds **3b** and **4b** (Figure 3).

The fluorescence of the fluorophore group of the three compounds is inhibited in the presence of the metal cations: Cu^{2+}, Ni^{2+} and Cr^{3+}. Most studies carried out for the detection of copper (II) by fluorescence show that the coordination of this metal ion results in an inhibition of the fluorescence emission of chromophoric groups [13]-[18]. Indeed, copper inhibits the

fluorescence of compounds **3b**, **4b** and **5b** through energy transfer and/or photoinduced electron transfer between the metal cation and the excited chromophore group. These two phenomenas may also be responsible for the decrease in fluorescence intensity in the presence of the metal cations Cr^{3+} and Ni^{2+}.On the other hand, after adding Zn^{2+} to compounds **3b**, **4b** and **5b**, we observe an increase in fluorescence intensity, allowing to consider the use of these compounds for the detection of zinc (II). Zinc (II) is a metal ion which has no redox tendency due to its electronic configuration d^{10}. This metal therefore cannot inhibit fluorescence by an electron transfer or energy transfer mechanism [19].

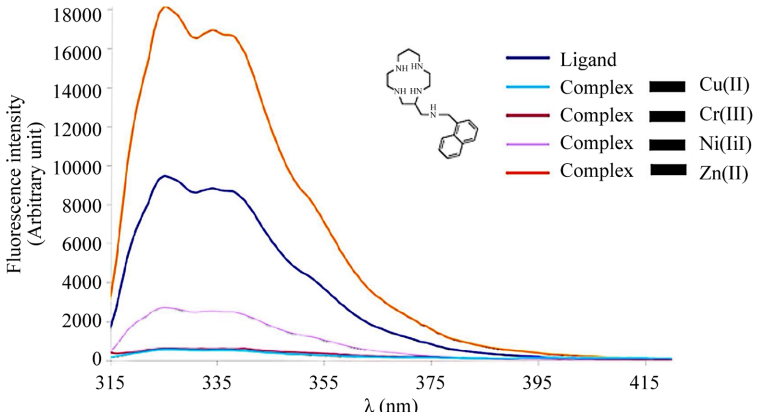

Figure 3. Emission spectra of complexes of compound **5b** in methanol, [10^{-5} M], λ_{ex} = 281 nm.

We therefore assume that the nitrogen atom of the exocyclic amine function of compounds (**3b**, **4b** and **5b**) is coordinated with zinc (II) according to the scheme shown in **Figure 4**.

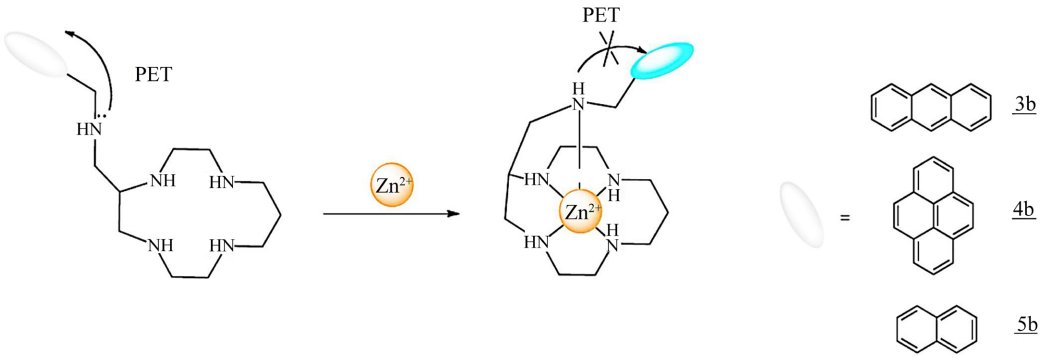

Figure 4. Coordination of Zn^{2+} by compounds: **3b**, **4b** and **5b.**

We carried out competitiveness tests with different cations in methanol in the presence of zinc (20 µM). Interferences caused by metal cations Na^{+}, Ca^{2+}, Al^{3+}, Ni^{2+}, Co^{2+}, Cd^{2+}, Hg^{2+} and Cu^{2+} (20 µM) were evaluated. The results obtained are shown in **Figure 5**.

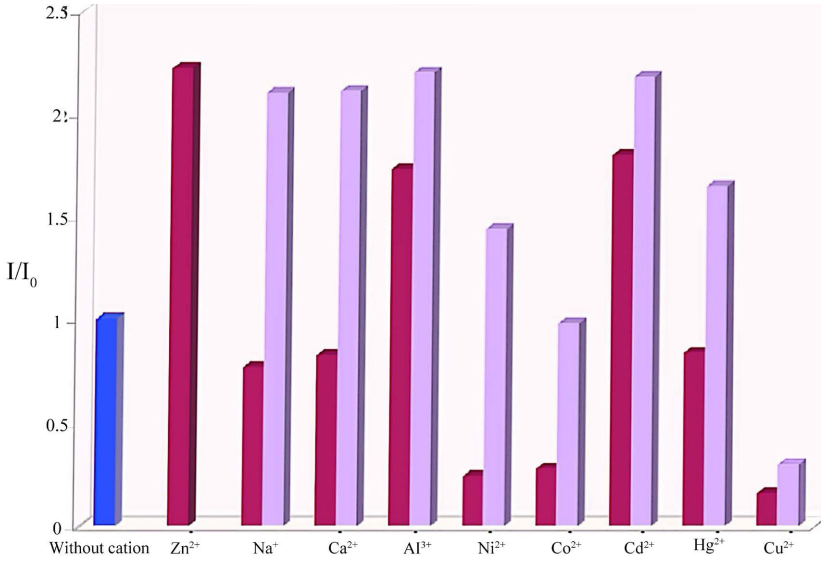

Figure 5. Fluorescence intensity of compound **3b** at 415 nm in methanol, in the presence of zinc(II) and different competitive cations. The metal cations Na^+, Ca^{2+}, Al^{3+} and Cd^{2+} show no significant interference at concentrations of 20 µM. On the other hand, the other metals induce a decrease in the fluorescence of the Zn^{2+} complex solution. This reduction in fluorescence intensity is of the order of 35% in the presence of Ni^{2+}, 44% in the presence of Co^{2+} and 26% in the presence of Hg^{2+}. The addition of Cu^{2+} results in a decrease in fluorescence of approximately 90% in the intensity of the zinc complex, probably due to a displacement of the zinc by the copper to form a more stable copper complex.

3.3. Physico-chemical Characterization of Metal Complexes

3.3.1. Characterization of Ni^{2+} Complexes

The spectra in solution of the nickel (II) complexes of compounds **3b**, **4b** and **5b** were recorded between 280 and 900 nm in methanol.

For the nickel complexes of compounds **3b**, **4b** and **5b**, we only observe a single transition band located in the visible range between 535 and 563 nm (the band expected at 340 nm is hidden by the strong absorption of the chromophoric groups), also characteristic of a hexacoordinated nickel (Table 1).

Table 1. Values of absorption maxima and molar extinction coefficients of different Ni^{2+}complexes in methanol.

Complex	λ_{max} (nm)	ε ($M^{-1}.cm^{-1}$)
$[Ni(\mathbf{2})]^{2+}$	340, 543	42, 14 [20]
$[Ni(\mathbf{3b})]^{2+}$	552	18
$[Ni(\mathbf{4b})]^{2+}$	535	88
$[Ni(\mathbf{5b})]^{2+}$	563	16

A UV-visible study of these complexes was performed in water (KCl, 0.1 M) as a function of pH. The band due to the d-d transition centered at a wavelength between 432 and 453 nm in an acidic environment ($2 < pH < 5$) is characteristic of a low-spin nickel of plan-square geometry. Above pH 5, the absorption band

is observed at a wavelength between 533 and 538 nm (which does not change even at pH 12) characteristic of the octahedral coordination geometry of a nickel complex (II) (**Table 2**) [10].

Table 2. Values of absorption maxima at different pH of the complexes of Ni^{2+} in H_2O, KCl (0.1 M).

Complex	pH [2 - 5] λ_{max} (nm)	pH [6 - 12] λ_{max} (nm)
Ni(**2**)]$^{2+}$	425	538 [2]
[Ni(**3b**)]$^{2+}$	436	537
[Ni(**4b**)]$^{2+}$	453	535
[Ni(**5b**)]$^{2+}$	432	533

This change in coordination geometry is observed by colorimetry. Indeed, we were able to distinguish the change in coloration of the Ni^{2+} complexes as a function of the pH: from the yellow color at acidic pH to purple color at basic pH (**Figure 5**).

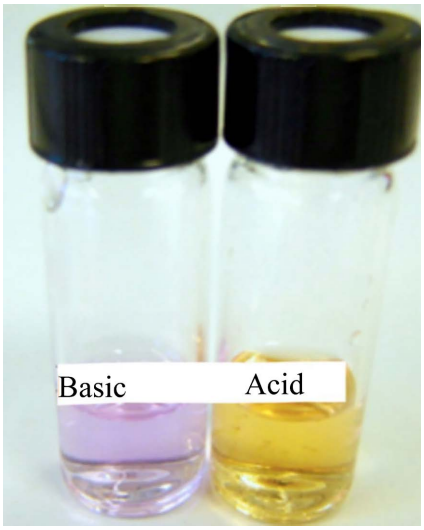

Figure 6. Change in color of aqueous solutions of Ni^{2+} complexes as a function of pH.

In order to be able to study the coordination geometry of Ni^{2+} by these different macrocycles, we carried out a study by fluorescence as a function of the pH in H_2O (KCl: 0.1 M). The results obtained for the complex [Ni(**3b**)] $(C_2H_3O_2)_2$ are shown in **Figure 6**.

The emission spectra of the Ni (II) complex as a function of pH show that an increase in pH leads to a decrease in the fluorescence intensity of the excited chromophoric groups (anthracene, pyrene and naphthalene). To explain this phenomenon, we compared the results we obtained with those described by Fabbrizzi *et al.* [10], who proposed a coordination scheme of Ni^{2+} by a similar

macrocycle (cyclam-based anthracene) (Scheme 2).

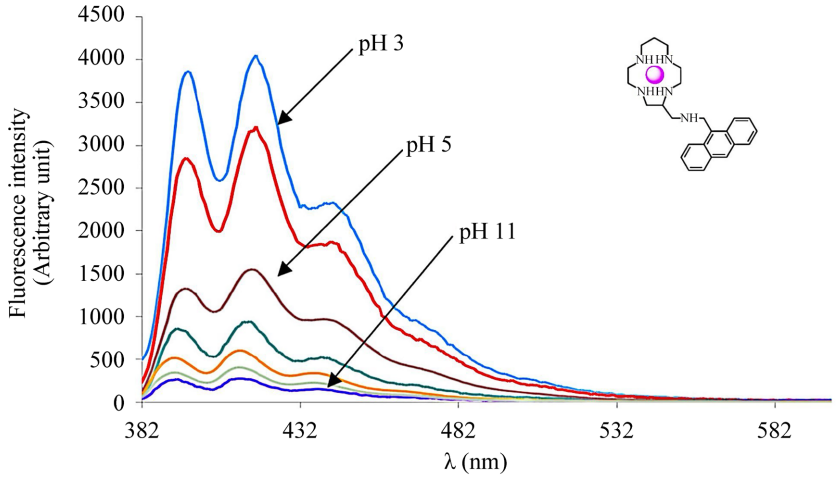

Figure 7. Evolution of the emission spectra of the complex [Ni(**3b**)] $(C_2H_3O_2)_2$ as a function of pH in H_2O, KCl (0.1 M).

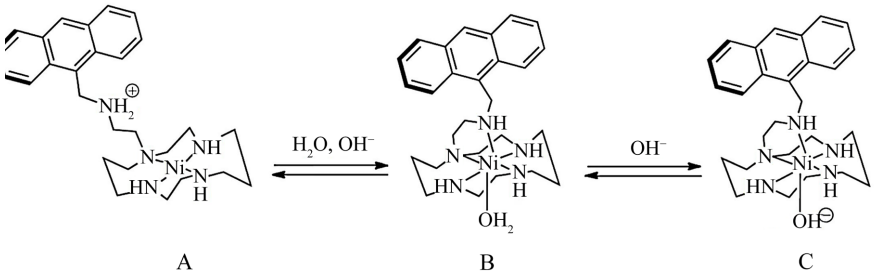

Scheme 2. Influence of pH on the coordination of amine function with nickel by a cyclam-based anthracene. [10]

Therefore, by correlating the results of UV-visible spectroscopy (Table 2) and the results of fluorescence as a function of pH, we can assume that the amine function of compound **3b** coordinates with nickel (II) and thus we propose an equilibrium scheme of protonation and deprotonation of the Ni^{2+} complex (Scheme 3).

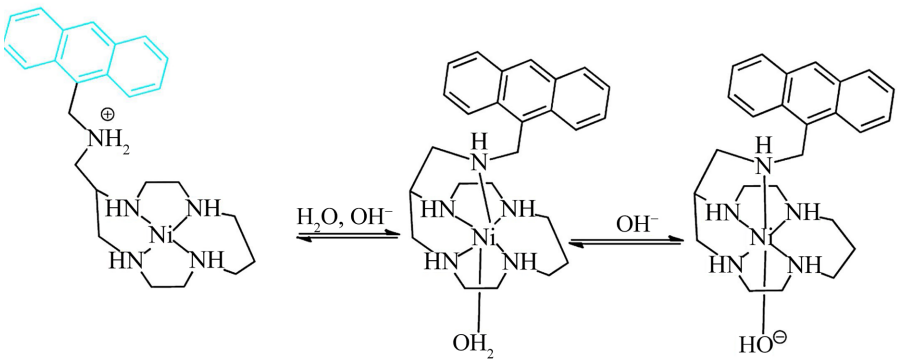

Scheme 3. Influence of pH on the coordiantion of amine function of the ligand 3b with nickel.

The Ni^{2+} complexes of compounds **4b** and **5b** have a photophysical behavior similar to the previous complex, on the other hand, a broadband appears at acidic pH at low energies (λ = 480 nm for the complex [Ni(**4b**)]$(C_2H_3O_2)_2$ and λ = 405 nm for the complex [Ni(**5b**)]$(C_2H_3O_2)_2$) which disappears in a basic environment (Figure 7). The presence of this band in an acidic medium can be explained by the formation of an intermolecular excimer due to electrostatic repulsions between the metal center and the protonated amine group [11].

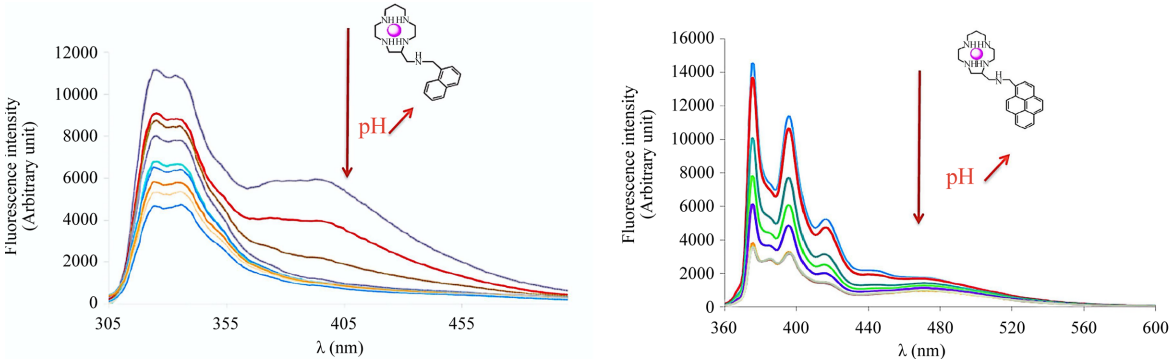

(a) (b)

Figure 8. Evolution of emission spectra as a function of pH in H_2O, KCl (0.1 M) of Ni^{2+} complexes of: (a)**4b** (λ_{ex} = 340 nm), (b)**5b** (λ_{ex} = 281 nm).

3.3.2. Characterization of Cu^{2+} Complexes

The UV-visible spectra of the copper (II) complexes of compounds **2** [20], **3b**, **4b** and **5b** were recorded in a solution of methanol. The maximum absorption of the broadband corresponding to the d-d transitions is between λ = 582 and 592 nm, these values are consistent with a pentacoordinated metal center [21] [22]. Table 3 shows the values of the maximum absorption bands of macrocycles metallized by $CuCl_2$.

Table 3. Values of absorption maxima and molar extinction coefficients of different complexes of Cu(II) in methanol.

Complex	λ_{max} (nm) d-d	ε ($M^{-1}.cm^{-1}$)
[Cu(**2**)Cl]Cl	582	145 [20]
[Cu(**3b**)Cl]Cl	582	147
[Cu(**4b**)Cl]Cl	596	230
[Cu(**5b**)Cl]Cl	585	215

The [Cu(**2**)Cl]Cl [20] and [Cu(**3b**)Cl]Cl complexes exhibit similar spectral characteristics, thus making it possible to conclude that they have the same coordination geometry. For the metal complexes [Cu(**4b**)Cl]Cl and [Cu(**5b**)Cl]Cl, the molar extinction coefficient is higher compared to the previous complexes. This increase may reflect a higher symmetry of the complex. The absorption bands correspond to the allowed transition (d_{xz}, d_{yz}→ d_{x2-y2}) and to the forbidden

transitions ($d_{xy} \rightarrow d_{x2-y2}$ and $d_{z2} \rightarrow d_{x2-y2}$) in C_{4v} symmetry.

We carried out UV-visible studies as a function of the pH of the [Cu(**L**)] $(NO_3)_2$ (**L** = **2**, **3b**, **4b** and **5b**) complexes in H_2O (KNO_3, 0.1 M) using HNO_3 (0.1 M) as the acid and NaOH (0.1 M) as the base (**Figure 8**). The superposition of the absorption spectra does not show a displacement of the copper d-d transition band but an increase in the molar extinction coefficient as the pH of the medium increases. This increase in the molar extinction coefficient can be explained by a low disturbance of the structure of the complex (while keeping the same coordination geometry). In this case, two hypotheses can be put forward:

In a basic environment, the amine function coordinates on the metal center. On the other hand, in an acidic environment, the amine protonates, causing it to move away from the copper and consequently, a molecule of the solvent coordinates on the metal.

The nitrogen atom of the amine group does not coordinate with copper at basic pH and the hyperchromic effect is due to the deprotonation of the water molecule coordinated with the metal center in the axial position. This is observed for all copper complexes and **Figure 9** shows the evolution of the absorption spectrum of the [Cu(**3b**)] $(NO_3)_2$ complex as a function of pH.

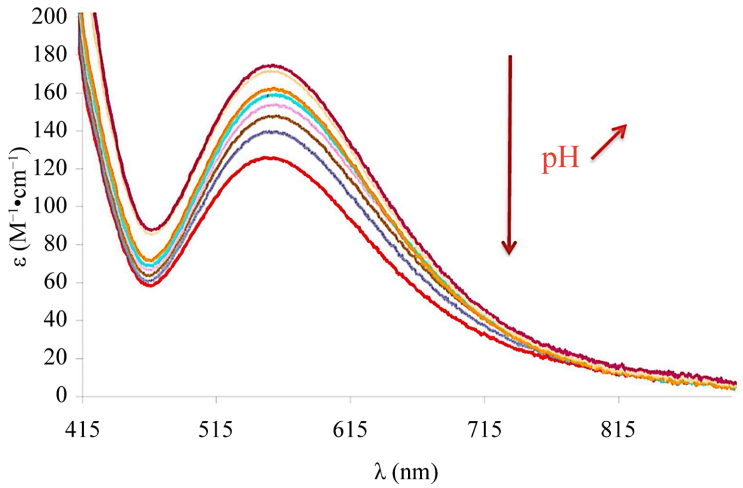

Figure 9. Evolution of the absorption spectrum of the compound [Cu(3b)]$(NO_3)_2$ ($2.5\ 10^{-3}$ M) in pH function in H_2O, KNO_3 (0.1 M).

Fluorescence studies in function of the pH of copper (II) complexes of compounds **3b**, **4b** and **5b** were performed at room temperature in H_2O (KCl: 0.1 M) using NaOH (0.1 M) as the base) and as acid HCl (0.1 M). The results obtained for the copper complex of compound **3b** are shown in **Figure 9**.

The superposition of the emission spectra as a function of the pH of the Cu complexes shows that the fluorescence intensity decreases in a basic medium. This disturbance allows us to propose the hypothesis of the coordination of the amine of the arm on the copper in a basic medium thus leading to the decrease in fluorescence by a mechanism of energy transfer and/or of photoinduced

electron transfer between the metal center and the excited chromophore group.

In the case of the copper complex of compound **4b** (Figure 10), we observe the appearance of a broad band centered at λ = 480 nm at acidic pH. This can be explained by the formation of an excimer form.

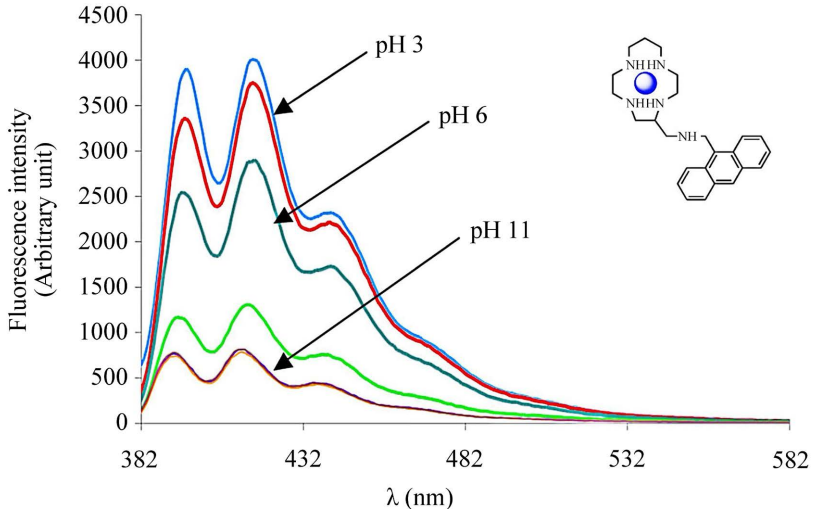

Figure 10. Evolution of the emission spectra as a function of the pH in H_2O, KCl (0.1 M) of the Cu^{2+} complex of compound **3b** (λ_{ex} = 345 nm).

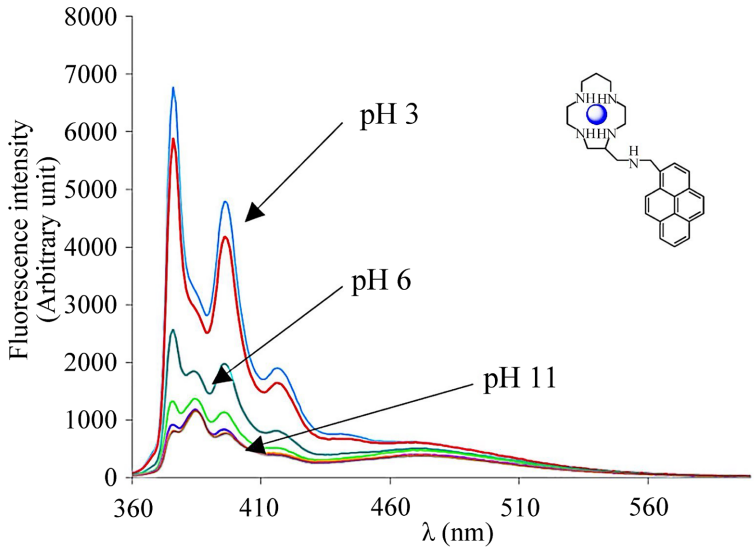

Figure 11. Evolution of the emission spectrum as a function of the pH of the Cu^{2+} complex of compound **4b**.

This hypothesis was confirmed by the crystallographic structure of this metal complex in the solid state (in its protonated form) obtained by X-ray diffraction (Figure 11).

In structure, copper is pentacoordinated by four nitrogen atoms of the macrocycle and one oxygen atom of a perchlorate ion. The presence of three perchlorate counter-ions confirms the protonated form of this complex.

Protonation of the exocyclic nitrogen atom of the copper (II) complex causes it to move away from the macrocycle by repulsive electrostatic effects and the formation of an excimer.

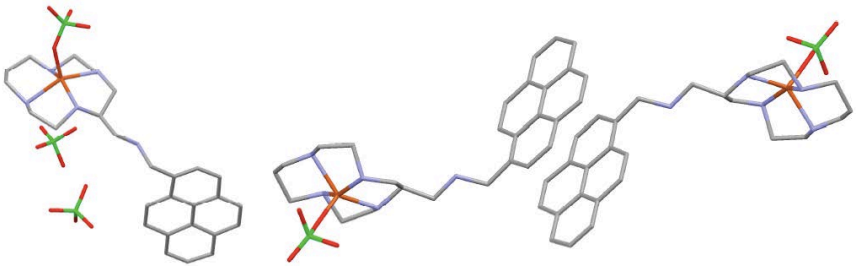

Figure 12. Crystallographic structure of the Cu complex of compound **4b**.

The RPE spectra of the Cu (II) complexes of compounds **3b**, **4b** and **5b** are recorded in X-band, that is to say at a frequency of about 9.3 GHz in frozen solution at 100 K in a methanol/toluene mixture (2/1). The spectra of the copper complexes are presented in **Figure 12**. The values of the parallel and perpendicular components ($g_{//}$, $g_{\perp}$) and of the hyperfine coupling constant ($A_{//}$) are reported and compared to the values obtained for the Cu (II) complexe of compound in **Table 4**.

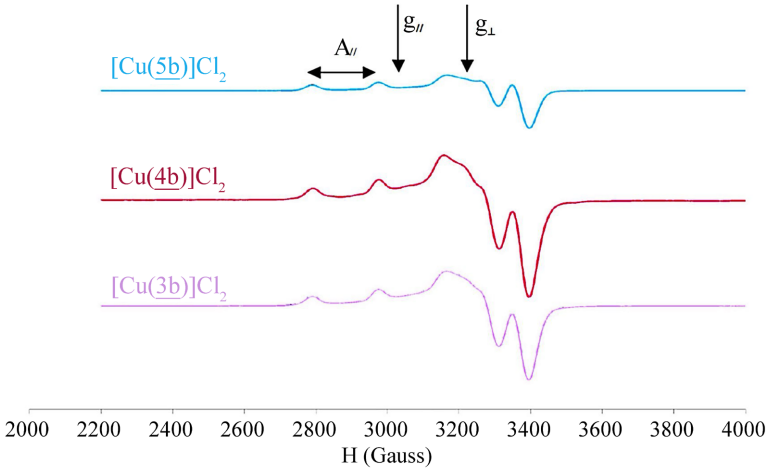

Figure 13. RPE spectra of different Cu^{2+} complexes recorded at 100 K in a methanol / toluene mixture (2/1).

Table 4. Values of $g_{\perp}$, $g_{//}$ and $A_{//}$ of different complexes of Cu^{2+} measured on the spectra RPE of these complexes.

Complex	g//	A//($\times 10^{-4}$ cm^{-1})	g⊥
[Cu(**2**)]Cl_2	2.187	192.2	2.068 [20]
[Cu(**3b**)]Cl_2	2.188	189.5	2.059
[Cu(**4b**)]Cl_2	2.190	188.8	2.058
[Cu(**5b**)]Cl_2	2.207	191.2	2.071

The spectra are characterized by a wide line associated with values of $g_{\perp}$ between 2.058 and 2.071 and four equidistant lines at weaker fields associated with values of $g_{//}$ between 2.18 and 2.21. The bursting of the $g_{//}$ component into four lines results from the hyperfine interaction with the copper nucleus of nuclear spin I = 3/2.

Likewise, the position of $g_{//}$ with respect to $g_{\perp}$ on the spectrum reflects the nature of the orbital which is occupied by the free electron. When the value of $g_{//}$ is greater than $g_{\perp}$, the single electron is located in the d_{x2-y2} orbital [22]. The values of $g_{//}$ and $g_{\perp}$ correspond to complexes of Cu^{2+} having a geometry pyramidal with a little distorted square base or an octahedral geometry axially elongated by the "Jahn-Teller" effect.

Spectra relating to mid-field transitions around 1600 Gauss were recorded for the different Cu^{2+} complexes at high enough concentrations in order to characterize the presence of forbidden spin transitions (ΔMs = 2) which can be induced by a dipolar coupling between two adjacent Cu^{2+} ions. **Figure 13** represents the two forbidden transitions observed for the complex [Cu(**5b**)]Cl_2 concentrated and diluted five times (the spectrum is similar to those obtained for the other complexes). The values of $g_{//}$ are reported in **Table 5**.

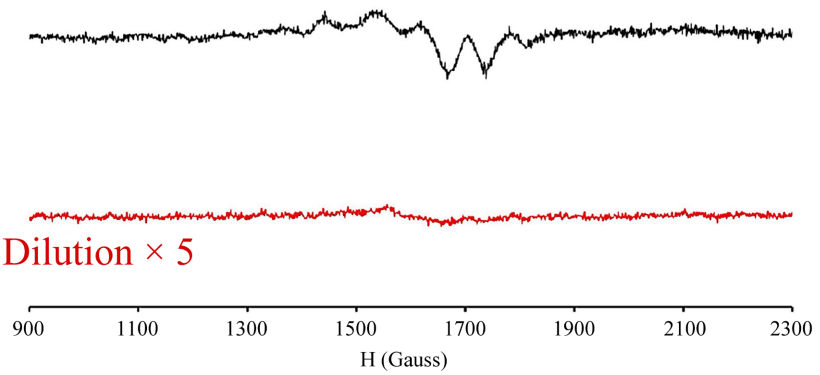

Figure 14. RPE spectrum relating to forbidden transitions of the complex [Cu(**5b**)]Cl_2 to different concentrations.

Table 5. RPE data relating to forbidden transitions of different Cu^{2+} complexes.

Complex	g//
[Cu(**2**)]Cl_2	4.187 [20]
[Cu(**3b**)]Cl_2	4.156
[Cu(**4b**)]Cl_2	4.232
[Cu(**5b**)]Cl_2	4.173

Spectra of forbidden transitions of different Cu complexes show the presence of dipolar coupling between adjacent copper atoms at high concentrations and its absence at lower concentrations. This can be explained by the formation of a coordinating dimer or polymer [20].

3.3.3. Characterization of Cr^{3+} Complexes

The UV-visible spectra of the different Cr^{3+} complexes of compounds **2**, **3b**, **4b** and **5b** were recorded in methanol and the results are shown in Table 6.

Table 6. Values of absorption maxima and molar extinction coefficients of different complexes of Cr^{3+} in methanol.

Complex	λ_{max} (nm)	ε ($M^{-1}.cm^{-1}$)
$[Cr(\mathbf{2})]^{3+}$	537	331 [20]
$[Cr(\mathbf{3b})]^{3+}$	537	330
$[Cr(\mathbf{4b})]^{3+}$	533	148
$[Cr(\mathbf{5b})]^{3+}$	534	123

Absorption bands due to d-d transitions of Cr^{3+} are observed at wavelengths between 533 and 537 nm, which is characteristic of a hexacoordinated chromium (III) complex [23] [24].

The molar extinction coefficients of chromium complexes generally distinguish the *cis* and trans isomers of chromium (III) [18]. The cis complexes of this metal cation often have higher extinction coefficients than those corresponding to the *trans* isomer.

The difference observed between the molar extinction coefficients of the different complexes (Table 6) can be explained by the *cis* conformations of the $[Cr(\mathbf{2})]^{3+}$ and $[Cr(\mathbf{3b})]^{3+}$ and *trans* complexes of the $[Cr(\mathbf{4b})]^{3+}$ and $[Cr(\mathbf{5b})]^{3+}$.

A study of the fluorescence as a function of the pH of the different Cr^{3+} complexes was carried out in H_2O (KCl, 0.1 M). The superposition of fluorescence emission spectra at different pH is shown in Figure 14.

We observe a decrease in the fluorescence intensity of the chromophoric groups of the Cr^{3+} complexes in a basic medium from a pH between 7 and 8 until it stabilizes at pH 12. These spectra are not similar to those obtained for the free ligands [9] (Figure 15).

The decrease in fluorescence with pH of chromium complexes may be due to the coordination of the metal center by the nitrogen atom of the exocyclic amine function of the macrocycle. In an acidic medium, this amine is protonated, thus causing it to move away from the macrocycle. Therefore, Cr-fluorophore interaction is minimized and fluorescence increases. In a basic medium, the

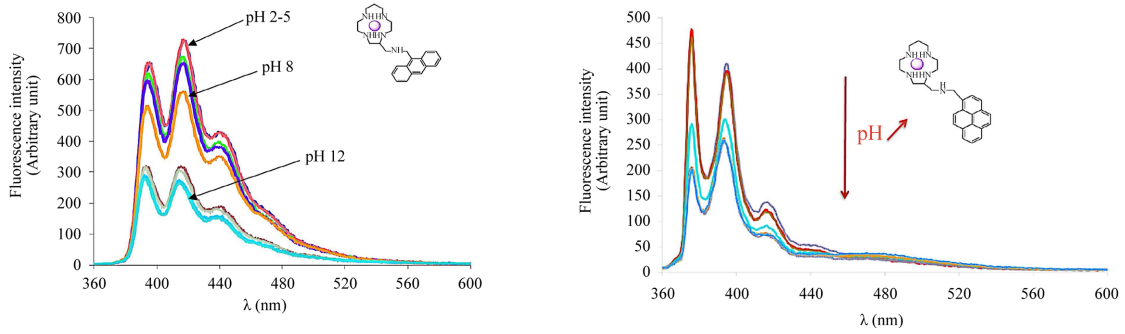

(a) (b)

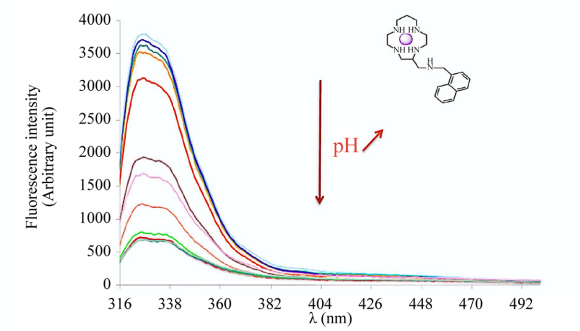

(c)

Figure 15. Evolution of emission spectra as a function of pH in H_2O, KCl (0.1 M) of the Cr^{3+} complexes of:(a)**3b** (λ_{ex} = 345 nm), (b)**4b** (λ_{ex} = 340 nm), (c) **5b** (λ_{ex} = 281 nm).

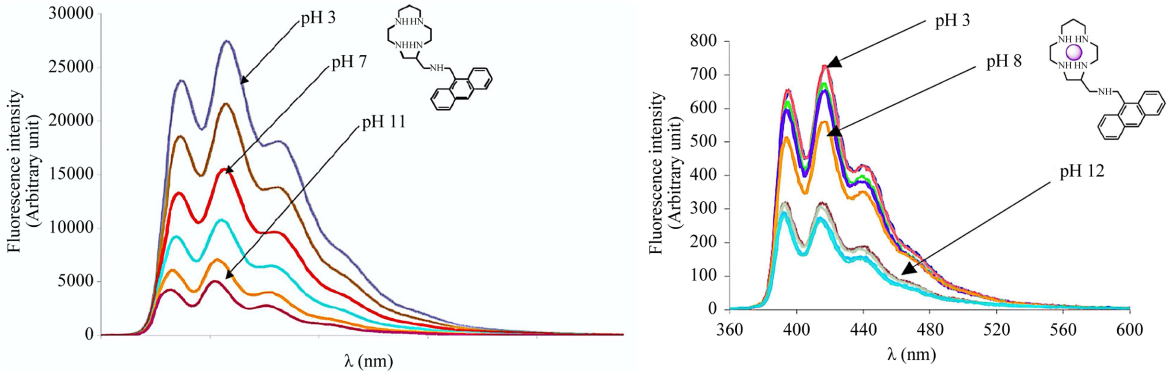

(a) (b)

Figure 16. Comparison of the emission spectra as a function of the pH of: (a) compound **3b**, (b) of the [Cr(**3b**)]Cl_3 complex.

nitrogen atom is deprotonated and coordinates with the metal center, thereby reducing the fluorescence of the fluorophore group excited by a mechanism of electron transfer and/or energy transfer between chromium and chromium chromophore group (**Figure 16**).

4. Conclusion

In this work, we focused on the synthesis of derivatives of 5-aminomethyl-[13]aneN_4 containing fluorophore groups (anthracene, pyrene and naphthalene) with the aim of designing new fluoro ionophores. Indeed, the coordination of cation metal by these compounds affects the fluorescence of the chromophore group. In the case of nickel(II), chromium(III) and zinc(II) complexes, we have been able to demonstrate through studies spectroscopic and spectrofluorometric that the metallic center is coordinated by the atom nitrogen of the functional group. On the other hand, in the structure of the copper (II) complex, copper is pentacoordinated by four nitrogen atoms of the macrocycle and one oxygen atom of a perchlorate ion. Protonation of the exocyclic nitrogen atom of the copper (II) complex causes it to move away from the macrocycle by repulsive

electrostatic effects and the formation of an excimer.

Conflicts of Interest

The authors declare no conflicts of interest.

References

[1] Huang, J. and Pu, K. (2021) Near-infrared Fluorescent Molecular Probes for Imaging and Diagnosis of Nephro-Urological Diseases. *Chemical Science*, **12**, 3379-3392. https://doi.org/10.1039/d0sc02925d

[2] Ji, S., Yang, J., Yang, Q., Liu, S., Chen, M. and Zhao, J. (2009) Tuning the Intramolecular Charge Transfer of Alkynylpyrenes: Effect on Photophysical Properties and Its Application in Design of off-on Fluorescent Thiol Probes. *The Journal of Organic Chemistry*, **74**, 4855-4865. https://doi.org/10.1021/jo900588e

[3] de Silva, A.P., Gunaratne, H.Q.N., Gunnlaugsson, T., Huxley, A.J.M., McCoy, C.P., Rademacher, J.T., *et al.* (1997) Signaling Recognition Events with Fluorescent Sensors and Switches. *Chemical Reviews*, **97**, 1515-1566. https://doi.org/10.1021/cr960386p

[4] Kim, M.H., Noh, J.H., Kim, S., Ahn, S. and Chang, S. (2009) The Synthesis of Crown Ether-Appended Dichlorofluoresceins and Their Selective Cu^{2+} Chemosensing. *Dyes and Pigments*, **82**, 341-346. https://doi.org/10.1016/j.dyepig.2009.02.004

[5] Callan, J.F., de Silva, A.P. and Magri, D.C. (2005) Luminescent Sensors and Switches in the Early 21st Century. *Tetrahedron*, **61**, 8551-8588. https://doi.org/10.1016/j.tet.2005.05.043

[6] Schmid, C., Neuburger, M., Zehnder, M., Kaden, T.A. and Hübner, T. (1998) Unexpected N-Configurations in a Ni^{2+} Complex of a Mono-N-Functionalized Macrocycle. *Polyhedron*, **17**, 4065-4070. https://doi.org/10.1016/s0277-5387(98)00210-1

[7] Tabushi, I., Taniguchi, Y. and Kato, H. (1977) Preparation of C-Alkylated Macrocyclic Polyamines. *Tetrahedron Letters*, **18**, 1049-1052. https://doi.org/10.1016/s0040-4039(01)92825-4

[8] Amendola, V., Fabbrizzi, L., Licchelli, M., Mangano, C., Pallavicini, P., Parodi, L., *et al.* (1999) Molecular Events Switched by Transition Metals. *Coordination Chemistry Reviews*, **190**, 649-669. https://doi.org/10.1016/s0010-8545(99)00110-1

[9] Jabri, R.Z., Rousselin, Y., Goze, C., Zrineh, A. and Denat, F. (2024) Synthesis and Photophysical Properties of a Novel [13] aneN_4 with Chromophoric Groups. *Open Access Library Journal*, **11**, e11587. https://doi.org/10.4236/oalib.1111587

[10] Fabbrizzi, L., Licchelli, M., Pallavicini, P. and Parodi, L. (1998) Controllable Intramolecular Motions That Generate Fluorescent Signals for a Metal Scorpionate Complex. *Angewandte Chemie International Edition*, **37**, 800-802. https://doi.org/10.1002/(sici)1521-3773(19980403)37:6<800::aid-anie800>3.0.co;2-u

[11] Jabri, R.Z., Lemeune, A., Zrineh, A. and Denat, F. (2023) Study of the Double Fluorescence of a New Anthracene (13) aneN_4. *Open Access Library Journal*, **10**, e10474. https://doi.org/10.4236/oalib.1110474

[12] Ferguson, J. and Tobe, M.L. (1970) Complexes of Chromium (III) with a Cyclic Tetradentate Secondary Amine. *Inorganica Chimica Acta*, **4**, 109-112. https://doi.org/10.1016/s0020-1693(00)93250-x

[13] Shnek, D.R., Pack, D.W., Arnold, F.H. and Sasaki, D.Y. (1995) Metal-Induced Dis-

persion of Lipid Aggregates: A Simple, Selective, and Sensitive Fluorescent Metal Ion Sensor. *Angewandte Chemie International Edition in English*, **34**, 905-907. https://doi.org/10.1002/anie.199509051

[14] Yang, R.-H., Chan, W.-H., Lee, A.W.M., Xia, P.-F. and Zhang, H.-K. (2003) A Ratiometric Fluorescent Sensor for Ag^{I} with High Selectivity and Sensitivity. *Journal of the American Chemical Society*, **125**, 2884-2885. https://doi.org/10.1021/ja029253d

[15] Boiocchi, M., Fabbrizzi, L., Licchelli, M., Sacchi, D., Vázquez, M. and Zampa, C. (2003) A Two-Channel Molecular Dosimeter for the Optical Detection of Copper (II). *Chemical Communications*, **2003**, 1812-1813. https://doi.org/10.1039/b305456j

[16] Zheng, Y., Gattás-Asfura, K.M., Konka, V. and Leblanc, R.M. (2002) A Dansylated Peptide for the Selective Detection of Copper Ions. *Chemical Communications*, **2002**, 2350-2351. https://doi.org/10.1039/b208012e

[17] Zheng, Y., Cao, X., Orbulescu, J., Konka, V., Andreopoulos, F.M., Pham, S.M., *et al.* (2003) Peptidyl Fluorescent Chemosensors for the Detection of Divalent Copper. *Analytical Chemistry*, **75**, 1706-1712. https://doi.org/10.1021/ac026285a

[18] Mei, Y., Bentley, P.A. and Wang, W. (2006) A Selective and Sensitive Chemosensor for Cu^{2+} Based on 8-Hydroxyquinoline. *Tetrahedron Letters*, **47**, 2447-2449. https://doi.org/10.1016/j.tetlet.2006.01.091

[19] Aoki, S., Kaido, S., Fujioka, H. and Kimura, E. (2003) A New Zinc (II) Fluorophore 2-(9-Anthrylmethylamino) Ethyl-Appended 1,4,7,10-Tetraazacyclododecane. *Inorganic Chemistry*, **42**, 1023-1030. https://doi.org/10.1021/ic020545p

[20] Jabri, R.Z., Rousselin, Y., Brandes, S., Goze, C., Zrineh, A. and Denat, F. (2023) Characterization and Structural Studies of Metal Complexes of 5-Aminomethyl-[13] $aneN_4$. *Open Access Library Journal*, **10**, e10829. https://doi.org/10.4236/oalib.1110829

[21] Rybak-Akimova, E.V., Nazarenko, A.Y., Chen, L., Krieger, P.W., Herrera, A.M., Tarasov, V.V., *et al.* (2001) Synthesis, Characterization, Redox Properties, and Representative X-Ray Structures of Four- and Five-Coordinate Copper(II) Complexes with Polydentate Aminopyridine Ligands. *Inorganica Chimica Acta*, **324**, 1-15. https://doi.org/10.1016/s0020-1693(01)00495-9

[22] El Ghachtouli, S., Cadiou, C., Déchamps-Olivier, I., Chuburu, F., Aplincourt, M. and Roisnel, T. (2006) (Cyclen- and Cyclam-Pyridine) Copper Complexes: The Role of the Pyridine Moiety in Cu^{II} and Cu^{I} Stabilisation. *European Journal of Inorganic Chemistry*, **2006**, 3472-3481. https://doi.org/10.1002/ejic.200600297

[23] Swisher, R.G., Brown, G.A., Smierciak, R.C. and Blinn, E.L. (1981) Chromium (III) Complexes Containing Macrocyclic Ligands. *Inorganic Chemistry*, **20**, 3947-3951. https://doi.org/10.1021/ic50225a069

[24] Hay, R.W. and Fraser, I. (1998) The Preparation and Kinetics of Aquation of Diastereoisomeric Complexes of *trans*-$[Cr(Me_8[14]aneN_4)Cl_2]^+$ ($Me_8[14]aneN_4$ = 3,5,7,7,10,12,14,14-Octamethyl-1,4,8,11-Tetra-Acyclotetradecane). *Polyhedron*, **17**, 1931-1936. https://doi.org/10.1016/s0277-5387(97)00488-9